Chapter 5

APPLICATIONS OF ANALYSIS TO MEASUREMENT

5.1 Method

Since one method of analysis is used throughout this section, it is here described in detail - description in the remainder of this section is restricted to that necessary to show the mode of application of the method to the particular measurement method.

All laboratory and field methods of measurement of inter-rill transport, with the exception of tracer methods, consist of a source area *from* which soil particles are transported and a collecting area *to* which they are transported. The extent to which transport and/or erosion has taken place during the rainfall event is gauged from the loss of mass from the source area or from the gain of mass in the collecting area.

The $\delta\theta$ method and its extension, the $\delta\theta\delta r$ method, can be applied here in exactly the same way as in Chapter 4. For a particular θ, or a particular θ and r (*i.e.* a particular direction and magnitude of displacement) it is first necessary to delineate the region on the source area that is capable of contributing material to the collecting area by means of the particular displacementsunder consideration. A function expressing the rate of transfer of material from the contributing region to the collecting area is obtained from the product of the mass transferred by each displacement, the area of the contributing region and the rate at which drop impacts (and therefore displacements) occur on the contributing region. This expression is a function of θ, or of θ and r, and the overall rate of transferral for all displacements capable of transferring material from the source to the collecting area is obtained by integrating the expression with respect to θ or θ and r, between appropriate limits. These latter are determined by the direction of the transport rate component required (*e.g.* integration between $\theta = -\pi/2$ and $\theta = \pi/2$ for the upslope component transport rate), and by source/collecting area geometrical constraints. The treatment in the remainder of this chapter will, for a particular measurement method, show by means of a figure the particular magnitude and direction of displacement being considered

and the resulting contributing region. The text will give the area of this region and give any constraints on the interval of integration. In all cases, the drop impact rate will be assumed to be i drop impacts per unit area per unit time, and the mass transferred for the one direction of displacement, θ, assumed to be $m\delta\theta/2\pi$ for the $\delta\theta$ method (Section 4.2.4) and $m(r,\theta)\cdot r\cdot\delta r\cdot\delta\theta$ for the $\delta\theta\delta r$ method (Section 4.3.2).

5.2 Laboratory Measurement

5.2.1 Splash cups

Consider a circular splash cup of radius R, where the total mass of soil particles splashed from the cup is used as a measure of the splash detachment. As the surface is always horizontal, the equation to the range line (equations (4.4), (4.5) and (4.6)) reduces to:

$$r = B ,$$

where

$$B = \frac{2v^2 \cos^2\alpha \tan\alpha}{g} ,$$

symbols as given in Section 4.2.3. For splash cup radii such that $2R \leqslant B$, all particles splashed into the air will fall outside the cup. The loss rate from the cup (or the collection rate outside the cup), c_1, is therefore given by:

$$c_1 = i\, m\, \pi\, R^2 . \qquad (5.1)$$

For $2R > B$, there are areas on the splash cup surface which are further than distance B from all or part of the splash cup edge. Some or all particles splashed from these areas return to the splash cup surface and thus are not collected on the surrounding area or registered as soil loss. The contributing region for such a situation is shown in Figure 5.1. It is

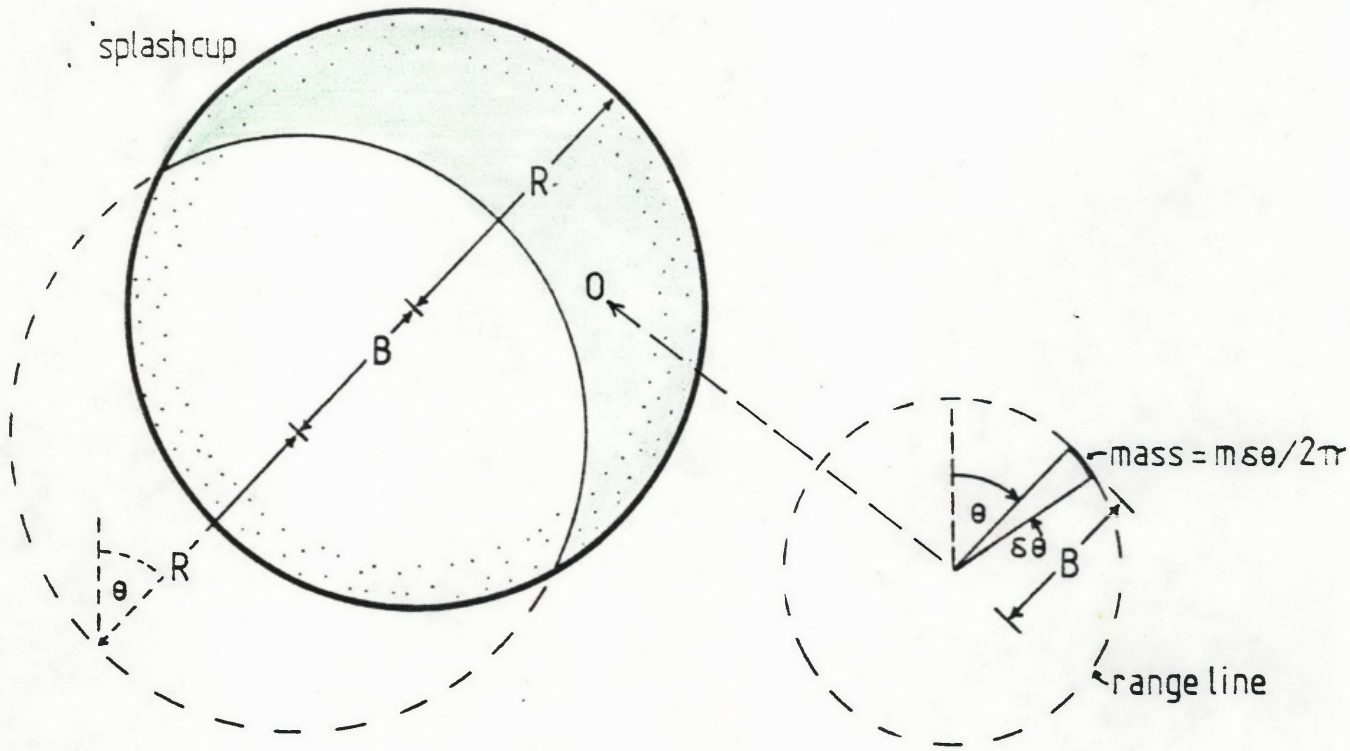

FIGURE 5.1: *Typical drop impact at O on the contributing region (green shading) of a splash cup. The contributing region is defined by the intersection of two circles of radius R with centres situated distance B apart in direction* θ.

defined by the intersection of two circles of radius R with centres situated distance B apart in direction θ, and its area is found as follows.

Consider two circles of radius R, $y = \sqrt{R^2 - x^2}$ with centre at $(0,0)$ and $y = \sqrt{R^2 - (x-B)^2}$ with centre at $(B,0)$ with $0 < B < 2R$ (using Cartesian x,y coordinates). The area of overlap between the two circles can be divided symmetrically into four equal regions by the x axis and the line $x = B/2$. The area of one of these regions is given by:

$$\int_{B/2}^{B} \sqrt{R^2 - x^2}\, dx = \frac{\pi R^2}{4} - \frac{R^2}{2} \sin^{-1} \frac{B}{2R} - \frac{B}{4} \sqrt{R^2 - B^2/4} .$$

The total area of overlap is therefore:

$$\pi R^2 - 2R^2 \sin^{-1} \frac{B}{2R} - B \sqrt{R^2 - B^2/4} .$$

The area of the region in each circle that is not overlapped by the other is:

$$2R^2 \sin^{-1} \frac{B}{2R} + B \sqrt{R^2 - B^2/4} . \qquad (5.2)$$

Thus the area of the contributing region is given by equation (5.2). The loss rate, c_2, from the splash cup is:

$$c_2 = \frac{im}{2\pi} \left(2R^2 \sin^{-1} \frac{B}{2R} + B \sqrt{R^2 - B^2/4}\right) \int_0^{2\pi} d\theta$$

$$= im\left(2R^2 \sin^{-1} \frac{B}{2R} + B \sqrt{R^2 - B^2/4}\right) . \qquad (5.3)$$

The rate at which soil is being splashed into the air over the whole splash cup is $im\pi R^2$, so that the ratio, P, of the weight of splashed soil lost from

the cup to the weight of soil actually detached and splashed into the air is given by:

$$P = \frac{2R^2 \sin^{-1} B/2R + B\sqrt{R^2 - B^2/4}}{\pi R^2}, \quad \text{for } 0 < B < 2R$$

$$P = 1, \quad \text{for } B \geq 2R . \qquad (5.4)$$

Since any radially symmetrical splash distribution can be characterised by masses m_i splashed onto annuli of radii B_i, and since for each B_i there is a P_i (given by equation (5.4), the ratio P_{total} for the splash distribution is given by:

$$P_{total} = \frac{\sum_i m_i P_i}{\sum_i m_i} .$$

Expressions for P have also been determined by Farrell *et al.* (1974):

for $a_1 > a_2$

$$P = \frac{2}{\pi}\left\{\frac{\pi X^2}{2} - 2\alpha^{*2}\left[\left(\frac{Y^2}{2} + \tfrac{1}{4}\right)\cos^{-1}Y - \frac{Y}{4}(1 + Y^2)^{\frac{1}{2}}\right]\right.$$

$$\pm \alpha^* u \cos u(1 - \alpha^{*2}\sin^2 u)^{\frac{1}{2}}$$

$$\left. \pm \left(\frac{\sin 2\phi}{4} + \frac{\phi}{2}\right)\right\} ,$$

for $a_1 \leq a_2$

$$P = (\alpha^* - 1)^2 + \frac{2}{\pi}\left\{\frac{X^2}{2} - 2\alpha^{*2}\left[\left(\frac{Y^2}{2} + \tfrac{1}{4}\right)\cos^{-1}Y - \frac{Y}{4}(1 - Y^2)^{\frac{1}{2}}\right]\right.$$

$$\pm \alpha^* u \cos u(1 - \alpha^{*2}\sin^2 u)^{\frac{1}{2}}$$

$$\left. \pm \left(\frac{\sin 2\phi}{4} + \frac{\phi}{2}\right)\right\} , \qquad (5.5)$$

where $Y = \frac{\alpha^{*2} + X^2 - 1}{2\alpha^* X}$,

$\phi = \sin^{-1}(\alpha^* \sin u)$,

a_1 = splash cup radius,

a_2 = splash circle (or range line) radius,

$\alpha^* = a_2/a$,

$X = x/a$,

x = distance between splash cup centre and splash circle centre, and

$u = \cos^{-1} Y$.

P_{total} for any splash distribution can be found in the same way as for equation (5.4).

The two functions for P (equations (5.4) and (5.5) can be evaluated for a range of values of B/R (= α^* of Farrell *et al.*). This is shown in Table 5.1. The close agreement between the values of the two functions suggests that they may be, in fact, identical, although proof of this by analytical means has not been attempted. Clearly, the expression for the ratio of measured splash loss to total splash detachment derived by the $\delta\theta$ method is simpler than that derived by Farrell's method.

TABLE 5.1: *Effect of ratio of B/R on ratio, P, of measured detachment to total detachment. Comparison of results of Farrell et al. (1974) with $\delta\theta$ method of this thesis*

B/R	Values of P $\delta\theta$ method - equation (5.4)	Values of P Farrell *et al.* (Figure 3) to nearest 0.01
0	0	0
0.25	0.16	0.15
0.50	0.31	0.32
0.75	0.47	0.46
1.00	0.61	0.61
1.25	0.74	0.75
1.50	0.86	0.86
1.75	0.95	0.94
≥2.00	1.00	1.00

This simplicity enables further analysis of the validity of splash cup measurements. As pointed out by Farrell *et al.*, equations (5.4) and (5.5) show that as the diameter of the splash cup is increased beyond the splash circle or range line radius, a decreasing fraction of the total splash detachment is collected outside the splash cup. As splash cups have generally been a standard size for experiments investigating the effect of drop kinetic energy on splash detachment, it is more useful to examine the effect of changing kinetic energy on the measured fraction of total detachment. There are three variables which could be affected by changes in the kinetic energy of the water drops causing particle displacement, *viz.* m, the mass detached by the drop impact; v, the velocity with which splashed particles are ejected and α, the splash angle. If the fraction, P, of total detachment splashed out of the splash cup is being considered, then m can be neglected, as this variable does not appear in the expression for P (equation (5.4)). There is no published experimental evidence as to how v and α vary with drop kinetic energy, but it could be assumed that, as the velocity of the falling water drop increases, the velocity, v, of ejection of splashed particles will increase. Figure 5.2 shows the effect of increasing v on the fraction, P, of total detachment splashed out of a standard 8.9 cm splash cup, as calculated from equation (5.4). Curves are shown for five values of α between 10° and 80°. From the high speed cinematography of Mutchler (1967), Levin and Hobbs (1971) and Ghadhiri and Payne (1978), 10° and 80° are the limits between which α can be expected to lie for most drop impact conditions. It can be seen from Figure 5.2 that, for ejection velocities greater than 1.6 ms^{-1}, the mass splashed out of the standard 8.9 cm splash cup is identical with the total mass detached. As ejection velocities decrease below 1.6 ms^{-1}, the measured fraction of the total detachment rapidly decreases. Thus, if ejection velocities vary systematically with drop impact velocity (and therefore drop kinetic energy), the fraction of total detachment collected outside the splash cup can also be expected to vary with drop kinetic energy. This introduces experimental artefact into any measured relationship between detachment and drop or rainfall kinetic energy.

5.2.2 Soil trays

Survey of Configurations

The most commonly used experimental set-up involves rectangular or square soil trays positioned horizontally or at a slope under a rainfall simu-

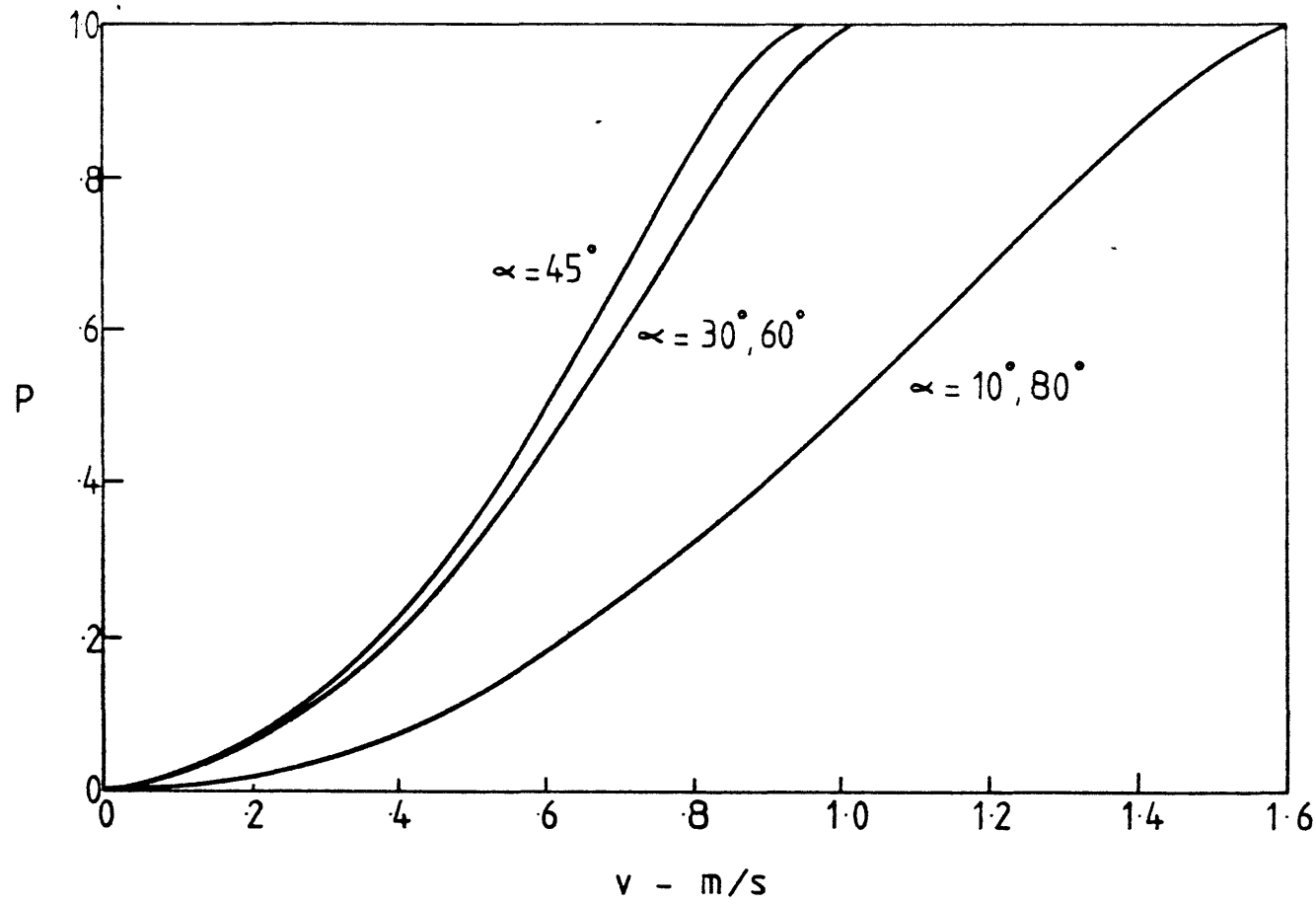

FIGURE 5.2: *Effect of velocity, v, of ejection of splashed particles on the measured fraction, P, of total detachment occurring on the splash cup surface.*

lator. As mentioned in Section 2.2.1, published reports show a wide variety of tray dimensions and source/collecting area geometries. In order that the analysis of such experimental systems be applicable to as many of them as possible, a survey of published experimental designs involving soil trays was made (Figure 5.3). It can be seen that source areas are generally rectangular in shape, while collecting areas have a more varied geometry.

The validity and utility of measurements using such experimental designs depends very much upon the fidelity with which the conditions and processes on the soil tray simulate those on a similarly shaped section of soil in the field. While it can be argued that comparative measurements of relative erodibilities of soil types may not require a high degree of fidelity, for measurements that seek to give an understanding of the way in which soil, moisture and drop factors affect inter-rill transport, or for those of a predictive nature, a high degree of fidelity is essential. Published experimental designs show that considerable care is taken in ensuring that simulated rainfall matches natural rainfall in its drop size and velocity characteristics, that soil drainage is similar to that in the field and that realistic rainfall intensities, soil slopes and antecedent conditions are used. Given this degree of care in simulating field conditions, it is worthwhile examining qualitatively the degree of similitude between inter-rill transport rates on a rectangular soil tray and on the same rectangle in the field.

Qualitative Considerations

For a rectangular area of soil within a large area of uniformly sloping soil surface, with vertical rainfall causing inter-rill transport, the two cross-slope component transport rates are equal and there is no net transport across slope. The downslope component transport rate exceeds the upslope component transport rate, so that the resultant transport rate is directed downslope. The magnitude and direction of this transport rate is represented by the arrows shown in Figure 5.4(a). There is no net erosion or deposition in the rectangle shown as the rate of transport into any given sub-area is the same as the rate of transport out of the sub-area.

Now consider the same rectangle of soil under exactly the same conditions, except that it is now in isolation, as for example, in a soil tray. The zone around the perimeter of the tray with a width equal to the magnitude

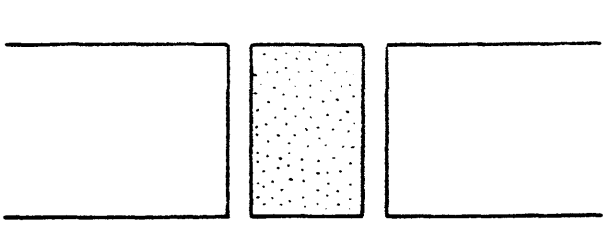

Moldenhauer and Koswara (1968)
slope - 9%

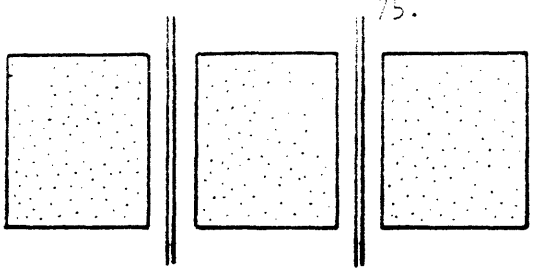

Lyles *et al.* (1969)
slope - 0°
Splash loss measured by weighing trays

Farmer and Van Haveren (1971)
slopes - 3%, 6%, 12%, 18%, 24%, 32%

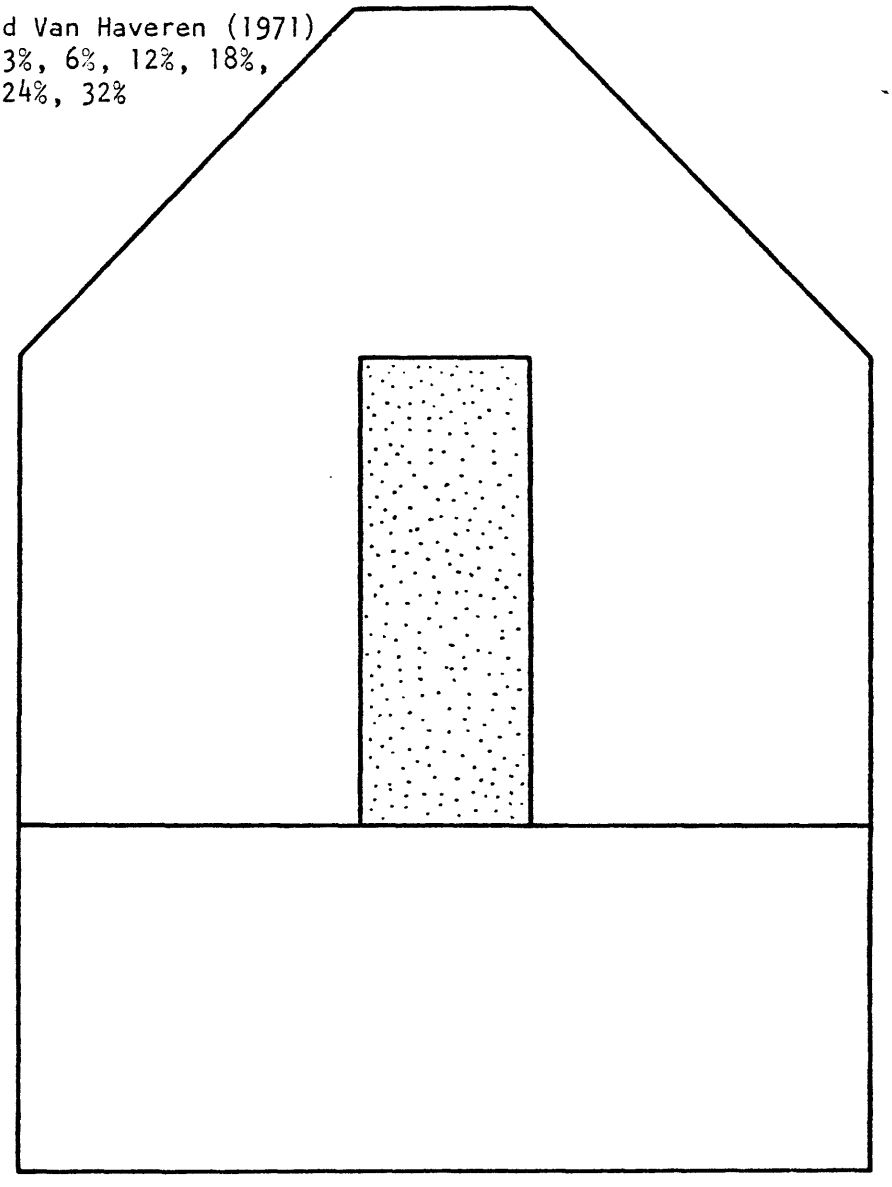

FIGURE 5.3: *Spatial configuration of source and collecting areas for studies using rectangular or square soil trays. Stippled area = source area; plain area = collecting area; single line = boundary over which splash can pass; double line = boundary of vertical extent preventing passage of splash.*

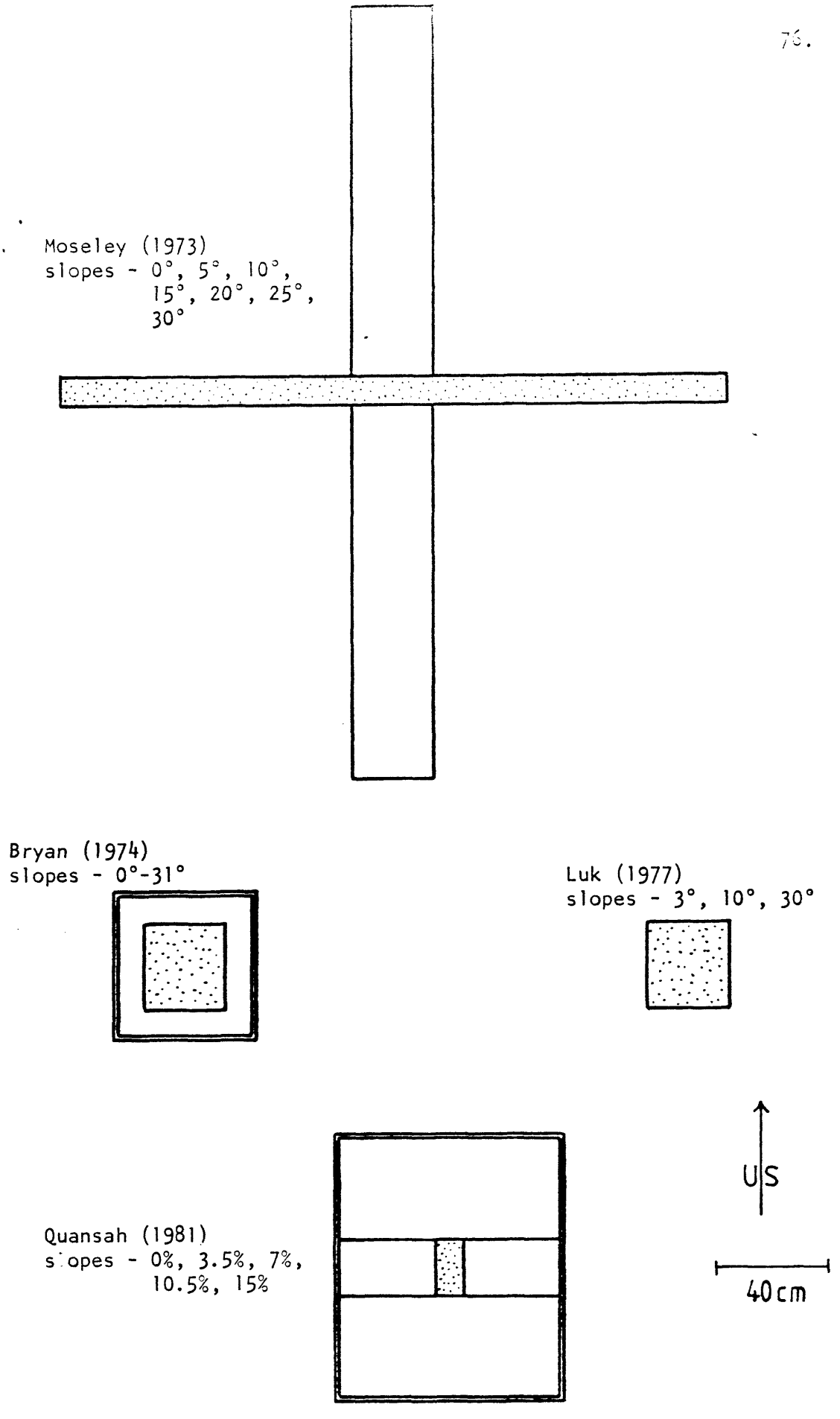

FIGURE 5.3: *continued.*

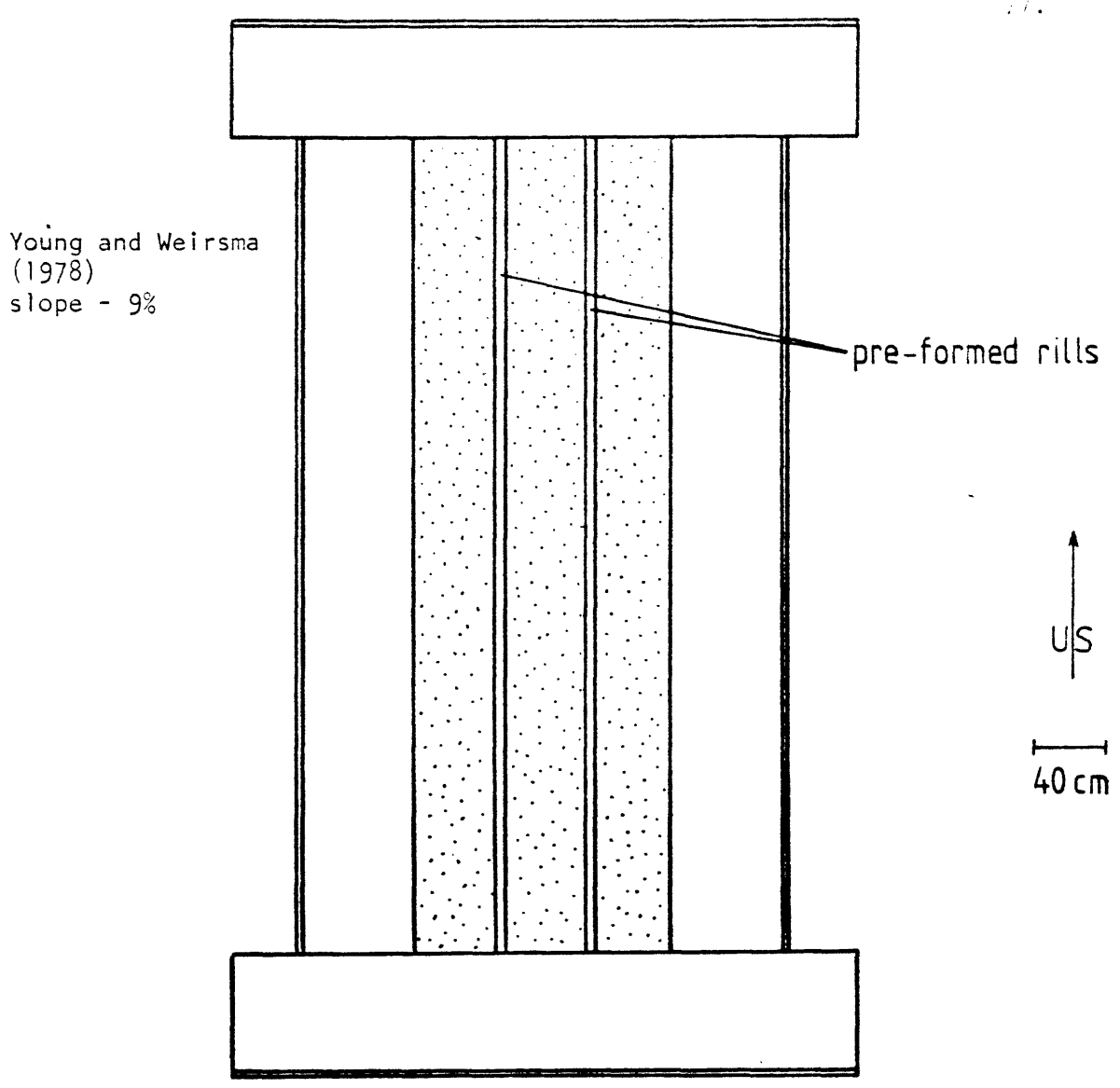

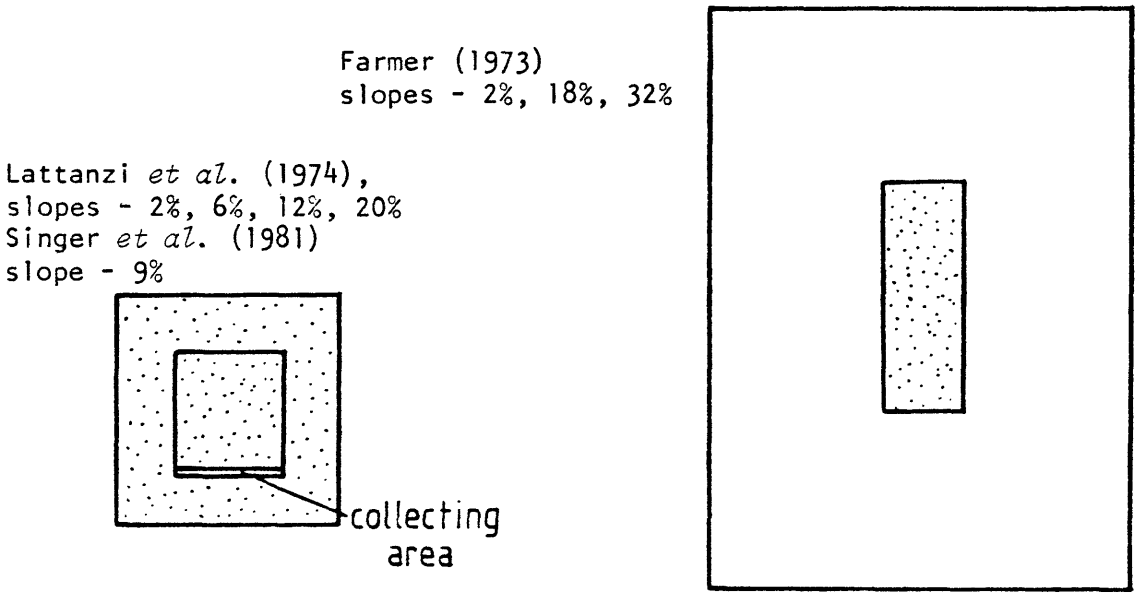

FIGURE 5.3: *continued.*

of the longest possible particle displacement is affected by the lack of soil beyond the tray boundary, *i.e.* some particle displacements across this zone, which would occur if the rectangle of soil was in the field, do not occur when the rectangle becomes isolated, as in a laboratory soil tray. If the dimensions of the tray are several times greater than the longest possible particle displacement, then there will be a central area where transport rates are unaffected (at least initially) by the abnormal transport rates of the perimeter zone (region A, Figure 5.4(b)).

At the centre of the downslope boundary, resultant transport can only be in one direction - downslope - as there is no particle movement in the upslope direction due to the lack of soil beyond the tray boundary. The resultant transport rate at this boundary is therefore equal to the downslope component transport rate, which is considerably larger than the resultant transport rate under field conditions. Similarly, the resultant transport at the centre of the sides and upslope boundary of the tray will be the cross-slope and upslope component transport rates respectively (Figure 5.4(b)). Soil particles crossing a point in the downslope right hand corner of the tray can only come from the upslope or left hand side of the point, so that the resultant transport is somewhere in the direction of the soil tray diagonal as shown in Figure 5.4(b). Furthermore, there will be a point on the soil tray where, due to insufficient source area on the upslope side, the downslope and upslope component transport rates will be equal, so that the resultant transport rate is zero.

Figure 5.4 shows that a rectangular area of soil, if brought into the laboratory and deprived of the source areas that surround it in the field, undergoes a change in the spatial disposition of resultant inter-rill transport rates. This change cannot be avoided by faithful duplication of soil, moisture and rainfall conditions - *it is inherent in the nature of the inter-rill transport process.* The role, then, of analysis as it applies to soil tray measurements, is to determine the relationship between the amounts of soil transported off the tray and the resultant transport rate were the rectangle of soil in the field under the same conditions.

Analysis of Total Loss Measurement

In the most common approach in the use of soil trays, the total mass splashed from the tray is used as a measure of the splash transport occurring

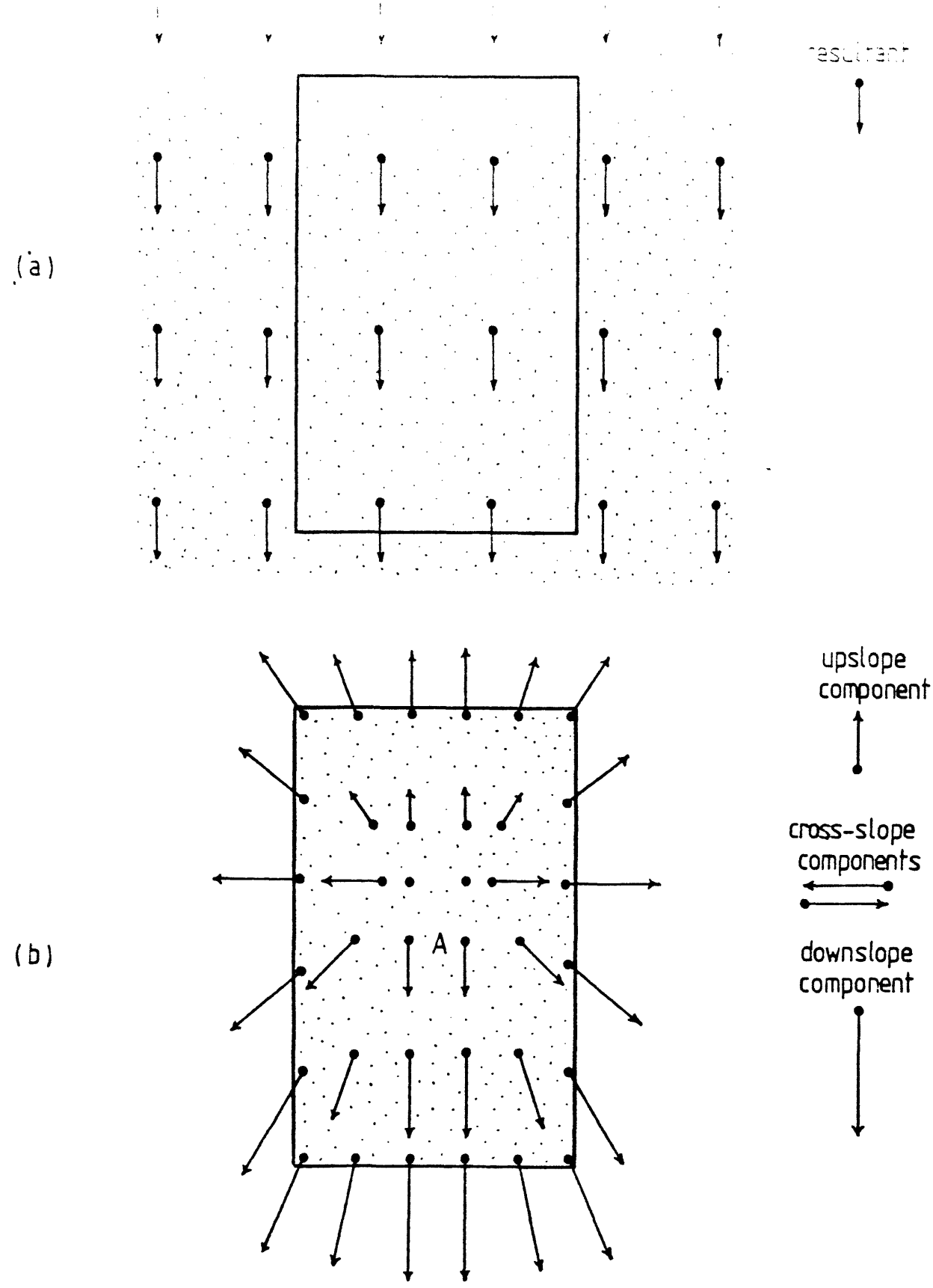

FIGURE 5.4: *Hypothetical spatial disposition of resultant inter-rill transport rates for:*
a) rectangular area of soil within a larger area of soil, i.e. field conditions;
b) the same rectangle of soil in isolation, i.e. as in a laboratory field tray.
Only in the region marked A is the resultant transport rate unaffected by the lack of source area outside the tray boundary and thus equal to the resultant transport rate under field conditions.

on the soil surface (*e.g.* Lyles *et al.*, 1969; Farmer, 1973; Bryan, 1974; Luk, 1977 - Figure 5.3). Analysis for the simplified representation follows a similar approach to that for the splash cup (Section 5.2.1).

Firstly consider a rectangular tray of dimensions such that the length and width projected on the horizontal plane are a and b respectively. The length of the diagonal is $\sqrt{a^2 + b^2}$. If this is less than the shortest particle displacement (B - C for the simplified representation - Section 4.2.2), then all displacements from all parts of the tray will result in particles landing outside the tray. The rate of splash collection, c_3, outside the tray is:

$$c_3 = i \cdot m \cdot b \cdot a \ . \qquad (5.6)$$

If the length of the diagonal of the tray is greater than the longest particle displacement (B + C for the simplified representation - Section 4.1.3), then it is not possible for all displacements from all parts of the tray to extend over the edge into the surrounding collecting area. This is illustrated in Figure 5.5. For $0 \leqslant \theta \leqslant \pi/2$, the area of the contributing region is (Figure 5.5(a)):

$$\begin{aligned} \text{area EFGLKJ} &= \text{area EFMJ} + \text{area KMGL} \\ &= (\text{length EF} \times \text{length FM}) + (\text{length MG} \times \text{length GL}) \\ &= bB\cos\theta + aB\sin\theta - (B^2 + aC)\sin\theta\cos\theta \\ &\quad + 2BC\cos^2\theta\sin\theta - bC\cos^2\theta - C^2\cos^3\theta\sin\theta \ , \end{aligned}$$

and the splash collection rate is therefore:

$$I_1 = \int_0^{\pi/2} \frac{im}{2\pi} \cdot \text{area EFGLKJ} \, d\theta$$

$$= \frac{im}{2\pi}\left[bB + aB - \frac{B^2 + aC}{2} - \frac{2BC}{3} - \frac{bC\tau}{4} - \frac{C^2}{4}\right] \qquad (5.7)$$

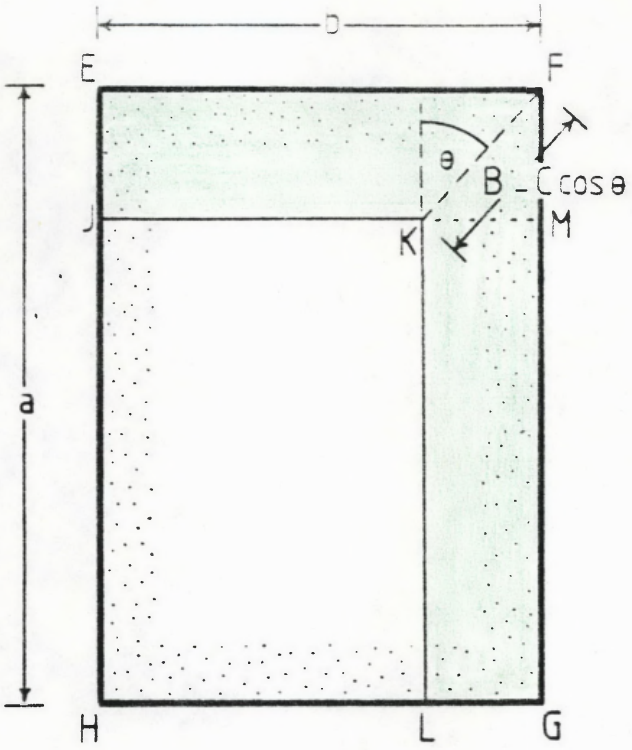

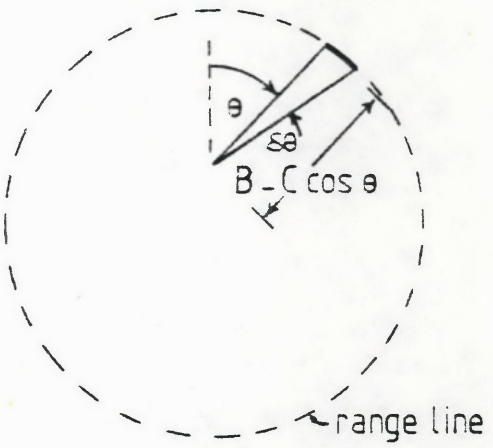

(a)

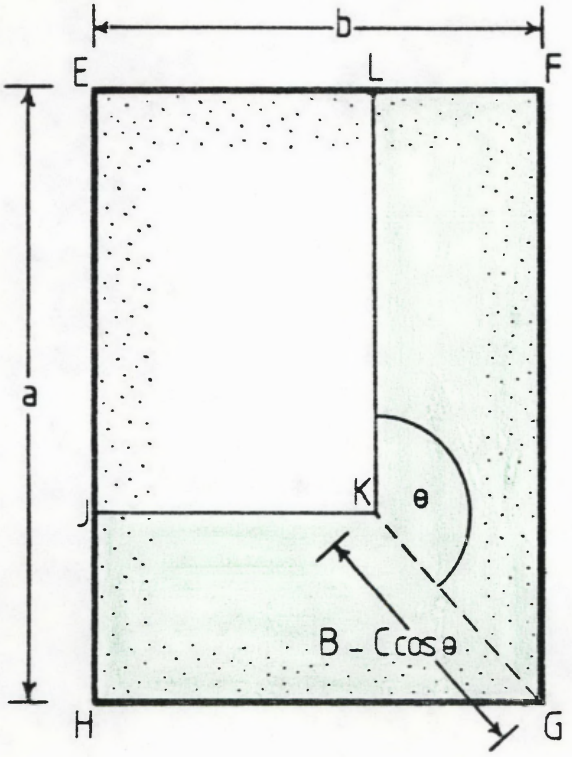

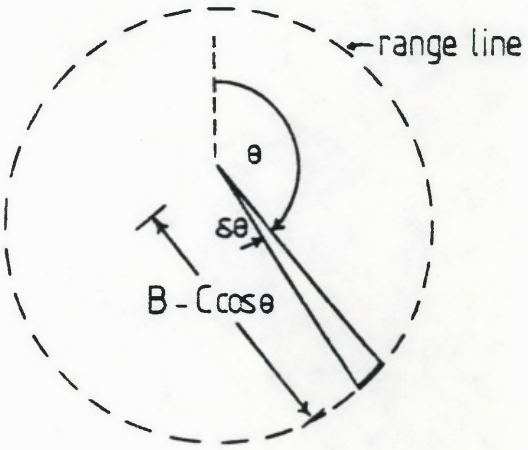

(b)

FIGURE 5.5: *Contributing regions (green shading) on a rectangular soil tray EFGH for:*
a) $-0 \leq \theta \leq \pi/2$; and
b) $\pi/2 \leq \theta \leq \pi$.

Exactly the same approach can be applied to displacements in the range of directions θ: $\pi/2 \leq \theta \leq \pi$. The contributing region is shown in Figure 5.5(b) - region LFGHJK.

$$\text{area LFGHJK} = -bB\cos\theta + aB\sin\theta + (B^2 - aC)\sin\theta\cos\theta - 2BC\cos^2\theta\sin\theta + bC\cos^2\theta + C^2\cos^3\theta\sin\theta .$$

The splash collection rate is given by the integral:

$$I_2 = \int_{\pi/2}^{\pi} \frac{im}{2\pi} \cdot \text{area LFGHJK}\, d\theta$$

$$= \frac{im}{2\pi}\left[bB + aB - \frac{B^2 - aC}{2} + \frac{2BC}{3} + \frac{bC\pi}{4} - \frac{C^2}{4}\right] \qquad (5.8)$$

From the symmetry of the range line about the upslope/downslope directions, the total collection rate or loss rate from the tray, c_4, for all displacement directions is obtained from equations (5.7) and (5.8):

$$c_4 = 2(I_1 + I_2)$$

$$= \frac{im}{\pi}\left[2B(a + b) - B^2 - \frac{C^2}{2}\right] \qquad (5.9)$$

or:

$$c_4 = \frac{im}{\pi}\left[B\rho - B^2 - \frac{C^2}{2}\right] \qquad (5.10)$$

where ρ is the length of the perimeter of the projection of the soil tray in the horizontal plane.

For the same rectangle of soil as defined by the boundaries of the soil tray, under similar conditions in the field, the component and resultant

splash transport rates are as given by equations (4.14) to (4.19) (Section 4.2.4). The rate of loss from the soil tray (equal to the collection rate, c_4, on the area surrounding the soil tray given by equations (5.6), (5.8) to (5.10) clearly bears no meaningful relationship to the component or resultant splash transport rates that would occur were the same rectangle of soil experiencing identical conditions in the field. Given a measurement of the magnitude of soil loss from a rectangular tray for a certain set of conditions, then only when the length of the soil tray diagonal is less than the shortest particle displacement (see discussion immediately prior to equation (5.6)) can any meaningful information be extracted from the measurement - *viz.* the mass displaced per drop, m, can be determined from equation (5.6) as the terms a,b and i are known or measureable.

The above analysis covers the cases $\sqrt{a^2 + b^2} \leqslant B - C$ and $\sqrt{a^2 + b^2} \geqslant B + C$. For intermediate tray dimensions, the range of θ over which the collecting rate expressions are integrated must be divided into two sub-ranges, for one of which the $\sqrt{a^2 + b^2} \leqslant B - C$ analysis applies, and for the other of which the $\sqrt{a^2 + b^2} \geqslant B + C$ analysis applies. This method of analysis is far more tedious as reference to the analysis preceding equation (5.12) below will show. Since, in terms of relationship to detachment or transport rates, the collecting rates thus obtained are similar to those obtained for $\sqrt{a^2 + b^2} \geqslant B + C$, this lengthy analysis is not given for all cases. The conclusions drawn for the $\sqrt{a^2 + b^2} \geqslant B + C$ case apply equally to the cases where $B - C \leqslant \sqrt{a^2 + b^2} \leqslant B + C$.

Types of Single Boundary Configuration

From Figure 5.3, it can be seen that the next most common source/collecting area configuration involves collecting splash passing over one boundary of the soil tray. There are three basic ways in which this can be done as illustrated in Figure 5.6. The collecting area can be narrower than (Figure 5.6(a)), of equal width to (Figure 5.6(b)) or wider than the source area. An example of the first configuration is that used by Moseley (1973); of the second, those used by Moldenhauer and Koswara (1968), Young and Weirsma (1973), Quansah (1981) and of the third, those used by Farmer and Van Haveren (1971), Young and Weirsma (1973), Young and Onstad (1978), Quansah (1981). These three configurations are henceforth termed single boundary configurations types 1, 2 and 3.

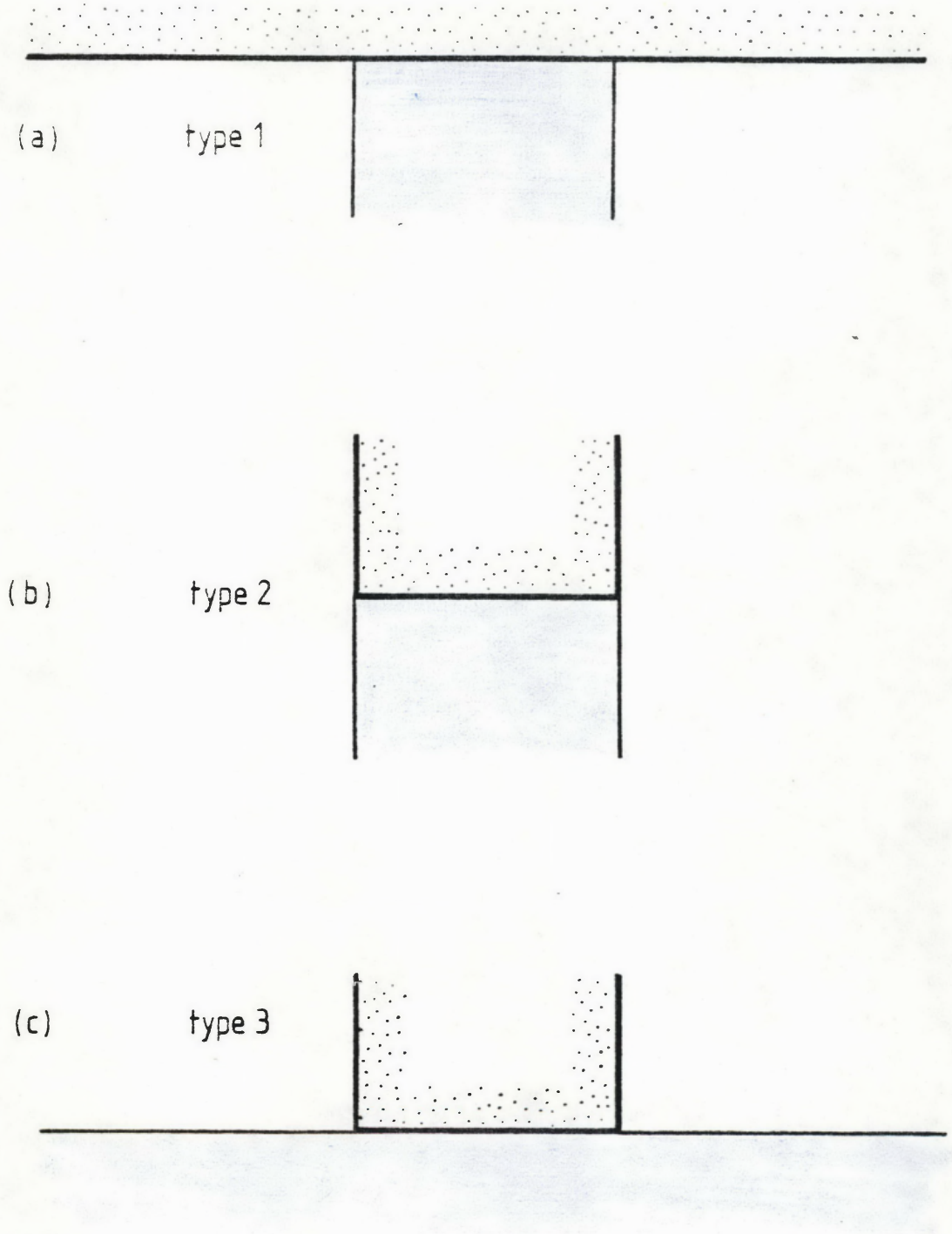

FIGURE 5.6: *Three basic types of single boundary source/ collecting area configurations:*
a) source area wider than collecting area;
b) source and collecting area of equal width;
c) collecting area wider than source area
(source areas stippled, collecting areas, blue shading).

Analysis of Single Boundary Configuration Type 1

The contributing region for this configuration is shown in Figure 5.7. The area of this region is:

$$\text{length EH} \times \text{length EF} = bC\cos^2\theta - bB\cos\theta \ .$$

The rate at which material passes from the source area to collecting area, *i.e.* collecting rate, c_5, is:

$$c_5 = \frac{im}{2\pi} \int_{\pi/2}^{3\pi/2} bC\cos^2\theta - bB\cos\theta \, d\theta$$

$$= i\ m\ b\ [\frac{B}{\pi} + \frac{C}{4}]$$

$$= i\ m\ [\frac{B}{\pi} + \frac{C}{4}] \quad \text{per unit of width of collecting area.} \qquad (5.11)$$

Comparison with equation (4.17) shows the collection rate per unit width of collecting area to be identical with the downslope component splash transport rate (not necessarily the rate on the tray but that applying if the rectangle of soil were returned to the field). Similar analysis to that above shows that similar source/collecting area configurations for the upslope end and sides of the tray will result in collecting rates per unit width of collecting area that are identical to the upslope and cross-slope component splash transport rates respectively.

The identity between collecting rates and component transport rates applies only if certain restrictions on the source/collecting area configuration are satisfied. The first of these is that distances AI and JB shown in Figure 5.7 (taking the configuration for the downslope component as an example) must be greater than $B - C\cos\theta$ when θ is close to $3\pi/2$ or $\pi/2$ respectively. If this is not the case, the area of the contributing region EFGH will not be given by $bC\cos^2\theta - bB\cos\theta$ for all θ. For θ

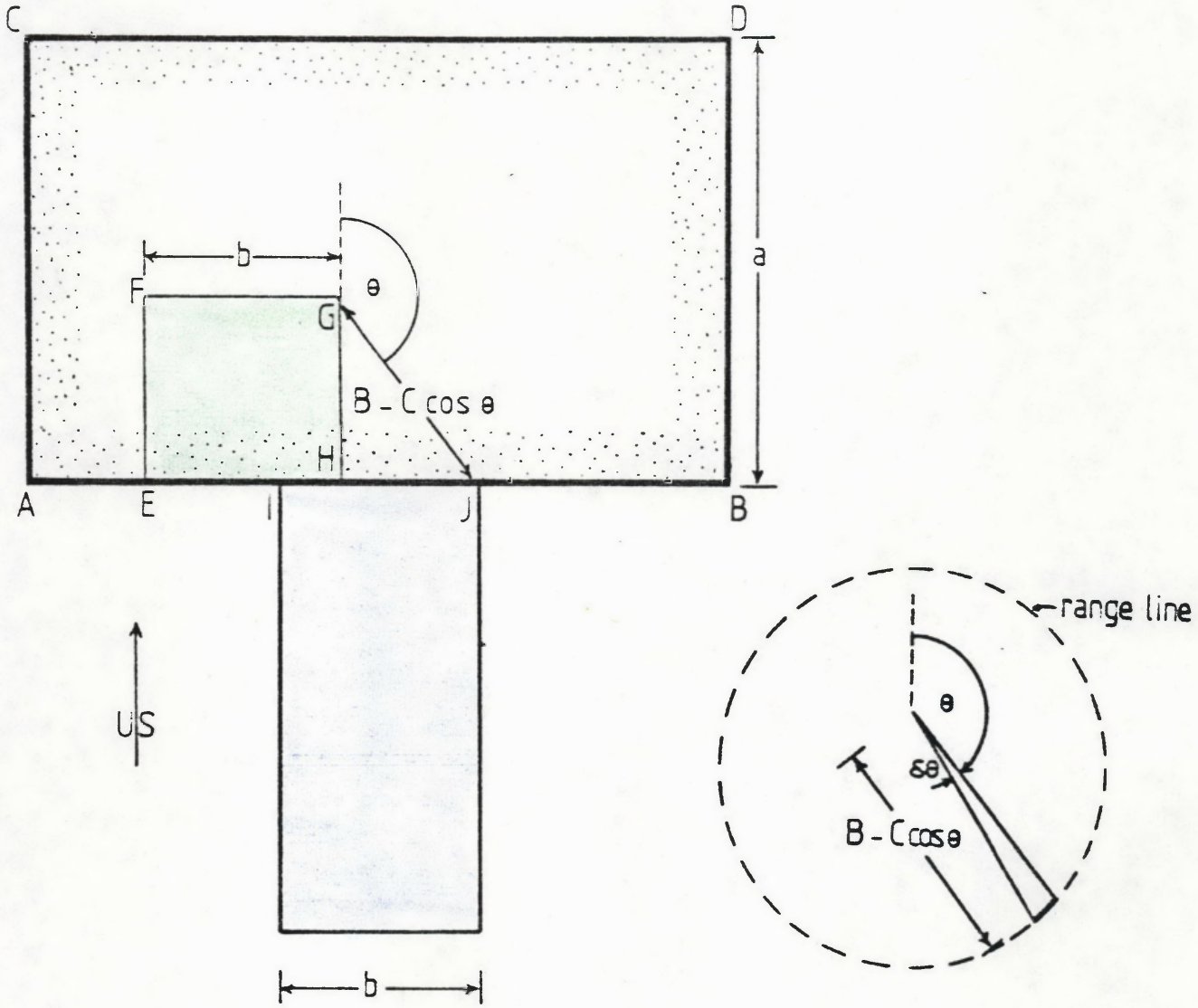

FIGURE 5.7: *Contributing region (green shading) for type 1 single boundary source/collecting area configuration. Source area - ABCD, collecting area - blue shading.*

close to $3\pi/2$ or $\pi/2$ the width of the contributing region will be less than b, due to the interference of the side of the tray. Analysis of the effect of this interference was not undertaken as in the only instance of the configuration (Moseley, 1973) the source tray is wide enough to avoid edge interference for all displacements less than 106 cm, which would include the majority of displacements. (Width of soil trays refers to the cross-slope dimension - Moseley's soil tray had a width of 2.4 m and a length of 10 cm.)

The second restriction to be placed on the derivation is that the length a of the tray must be greater than $B - C\cos\theta$ when θ is in the region of π, *i.e.* must be greater than $B + C$. If not, the contributing region EFGH (Figure 5.7) will be restricted by the upslope edge of the soil tray when θ is close to π. The configuration of Moseley (1973) with a tray length of 10 cm (less than a substantial proportion of particle displacements) does not comply with this restriction, so analysis of the effect of this is given below.

Figure 5.8 shows that, for θ changing in value from $\pi/2$ to π, the contributing region is firstly fully within the source tray (Figure 5.8(a)), then comes a critical value of θ, termed θ_c, when the contributing region upslope and downslope boundaries coincide with those of the soil tray (Figure 5.8(b)). For $\theta > \theta_c$ the contributing region is restricted in length to that of the soil tray, despite the potential contributing region being of greater length (Figure 5.8(c)). The areas of the contributing regions are:

$$\frac{\pi}{2} \leqslant \theta < \theta_c ,$$

$$\text{length EF} \times \text{length FG} = bC\cos^2\theta - bB\cos\theta$$

$$\theta_c \leqslant \theta \leqslant \pi ,$$

$$\text{length EF} \times \text{length FG} = ab .$$

The collecting rate for θ: $\pi/2 \leqslant \theta \leqslant \pi$ is given by the integral:

$$I_1 = \frac{imb}{2\pi} \int_{\pi/2}^{\theta_c} C\cos^2\theta - B\cos\theta \, d\theta + \frac{imb}{2\pi} \int_{\theta_c}^{\pi} a \, d\theta .$$

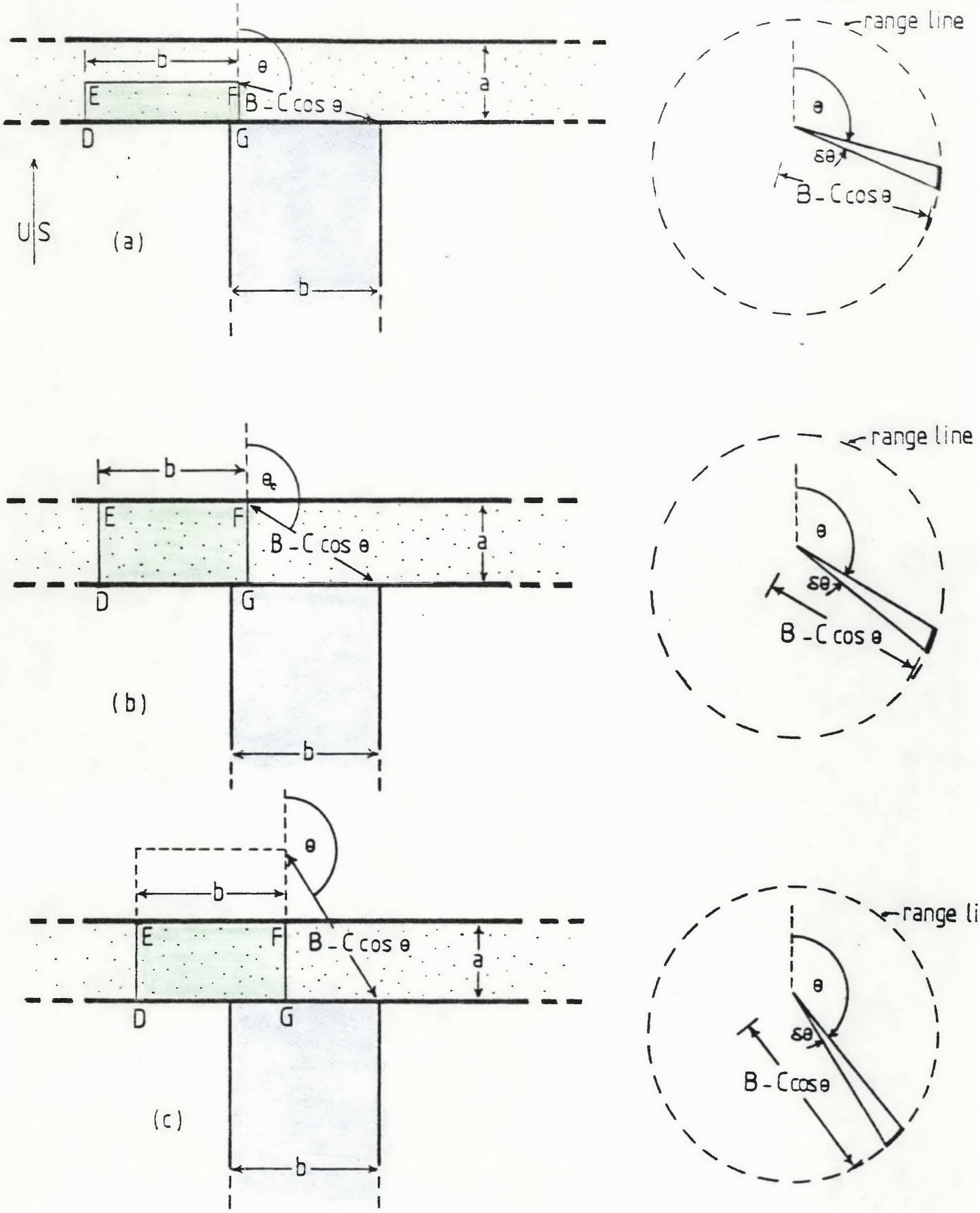

FIGURE 5.8: *Contributing regions (green shading) for type 1 single boundary source/collecting area configuration with length of source area less than the length of some particle displacements:*
a) $\pi/2 \leq \theta \leq \theta_c$; *b)* $\theta = \theta_c$; *c)* $\theta_c \leq \theta \leq \pi$.
Source area stippled; collecting area, blue shading.

θ_c can be obtained from the trigonometry of Figure 5.8(b) where:

$$(B - C\cos\theta_c)\cos(\pi - \theta_c) = a \ ,$$

from which:

$$\cos\theta_c = \frac{B \pm \sqrt{B^2 + 4aC}}{2C} \ .$$

Discarding the positive root (as $\pi/2 \leqslant \theta_c \leqslant \pi$) gives:

$$\theta_c = \cos^{-1}\frac{B - \sqrt{B^2 + 4aC}}{2C} \ ,$$

whereupon the integral above can be evaluated to give:

$$I_1 = \frac{imbC}{4\pi}\cos^{-1}\frac{B - \sqrt{B^2 + 4aC}}{2C} + \frac{imbC}{8\pi}\sin 2\cos^{-1}\frac{B - \sqrt{B^2 + 4aC}}{2C}$$

$$- \frac{imbC}{8} - \frac{imbB}{2\pi}\sin\cos^{-1}\frac{B - \sqrt{B^2 + 4aC}}{2C} + \frac{imbB}{2\pi}$$

$$+ \frac{imab}{2} - \frac{imab}{2\pi}\cos^{-1}\frac{B - \sqrt{B^2 + 4aC}}{2C} \ . \qquad (5.12)$$

To determine the total collection rate for all displacements with a downslope component (*i.e.* for θ: $\pi/2 \leqslant \theta \leqslant 3\pi/2$), the corresponding integral for θ: $\pi \leqslant \theta \leqslant 3\pi/2$ should be evaluated. For the purposes, however, of calculating collection rates for the specific configuration used by Moseley, numerical integration provides a preferable alternative to the evaluation of lengthy trigonometric expressions. It suffices here to point out that the integral I_1 of equation (5.12) bears no meaningful relationship to the partial downslope component splash transport rate of θ: $\pi/2 \leqslant \theta \leqslant \pi$, which, being half of the total downslope component splash transport rate (θ: $\pi/2 \leqslant \theta \leqslant 3\pi/2$) is given by:

$$i\ m\ b\ [\frac{B}{2\pi} + \frac{C}{8}] \ .$$

Note, however, that Moseley's configuration, because of the narrow soil tray and the position of the collecting areas, would give a reasonable, if slightly imperfect, estimate of detachment.

Analysis of Single Boundary Configuration Type 2

The contributing region for this configuration of source/collecting areas is shown in Figure 5.9. The area of the contributing region is:

$$\text{length DE} \times \text{length DG} = \text{length DE} \times (\text{length DH} - \text{length GH})$$

$$= -bB\cos\theta + bC\cos^2\theta + B^2\sin\theta\cos\theta - 2BC\cos^2\theta\sin\theta + C^2\cos^3\theta\sin\theta \ .$$

This expression holds only for θ: $\pi/2 \leqslant \theta \leqslant \pi$. Integration between these limits yields the collection rate for this range of θ, thus:

$$I_1 = \frac{im}{2\pi}\left[bB + \frac{bC\pi}{4} - \frac{B^2}{2} - \frac{2BC}{3} - \frac{C^2}{4}\right] \ .$$

For the range of θ, $\pi \leqslant \theta \leqslant 3\pi/2$, appropriate modification of Figure 5.9 enables the determination of an expression for the area of the contributing region from which the collecting rate can be derived as previously, thus:

$$I_2 = \frac{im}{2\pi}\left[bB + \frac{bC\pi}{4} - \frac{B^2}{2} - \frac{2BC}{3} - \frac{C^2}{4}\right] \ .$$

The total collection rate, c_6, for all displacements with a downslope component (θ: $\pi/2 \leqslant \theta \leqslant 3\pi/2$) is therefore:

$$c_6 = I_1 + I_2 = \frac{im}{\pi}\left[bB + \frac{bC\pi}{4} - \frac{B^2}{2} - \frac{2BC}{3} - \frac{C^2}{4}\right] \ . \qquad (5.13)$$

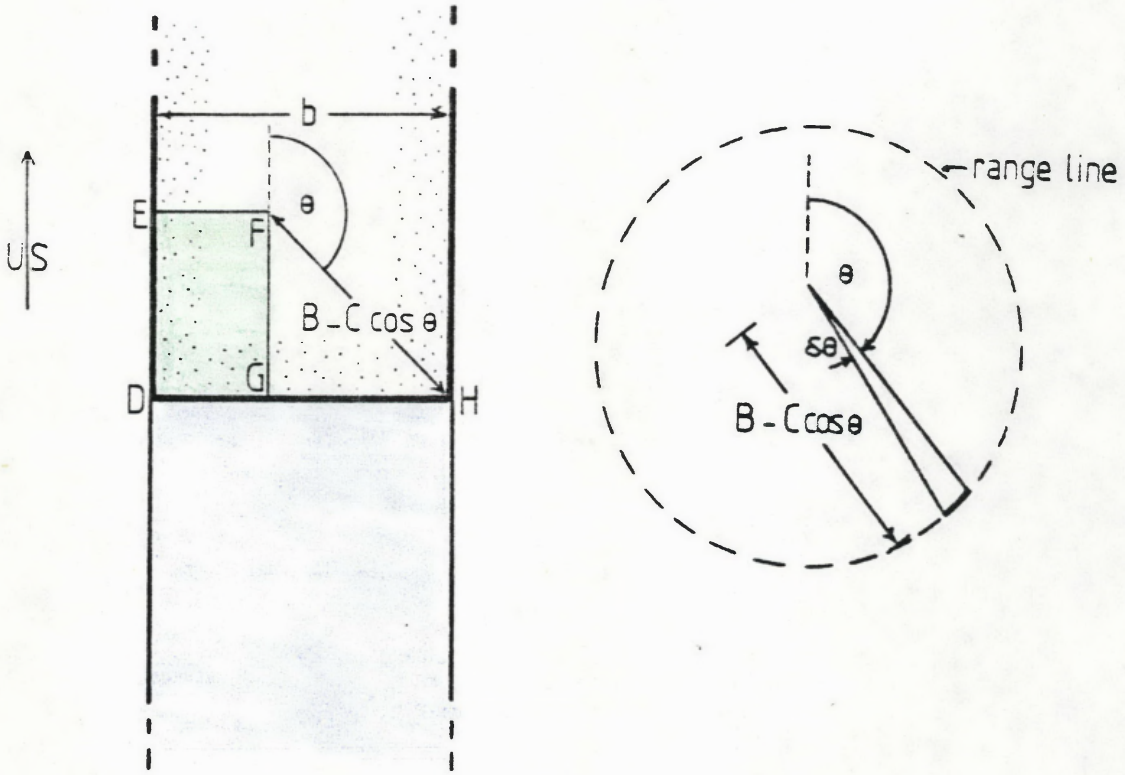

FIGURE 5.9: *Contributing region (green shading) for type 2 single boundary source/collecting area configuration. Source area stippled; collecting area, blue shading.*

Comparison of this equation with equations (4.14) to (4.19) shows that there is no meaningful relationship between the rate of collection of splash in the collecting area at the downslope end of the soil tray and any of the corresponding field component or resultant splash transport rates. As for the previous configuration, a tray length shorter than B + C will limit the upslope/downslope dimension of the contributing region on the tray. As, however, the collection rate for the unrestricted case above is already unrelated to any component or resultant transport rates, analysis of this effect has not been undertaken.

Analysis of Single Boundary Configuration Type 3

The contributing region for this configuration of source/collecting areas is shown in Figure 5.10. The area of the contributing region is:

$$\text{length DE} \times \text{length DG} = bC\cos^2\theta - bB\cos\theta \ .$$

The collection rate, c_8, for all displacements with downslope component is:

$$c_8 = \frac{im}{2\pi} \int_{\pi/2}^{3\pi/2} bC\cos^2\theta - bB\cos\theta \, d\theta$$

$$= i \ m \ b \ [\frac{B}{\pi} + \frac{C}{4}]$$

$$= i \ m \ [\frac{B}{\pi} + \frac{C}{4}] \quad \text{per unit width of source area.}$$

(5.14)

Comparison with equation (4.17) shows the collecting rate per unit width of source area to be identical with the corresponding field downslope component splash transport rate. Similar analysis to that above shows that similar source/collecting area configurations for the upslope end and sides of the tray will result in collecting rates per unit width of source area that are identical to the upslope and cross-slope component splash transport rates respectively.

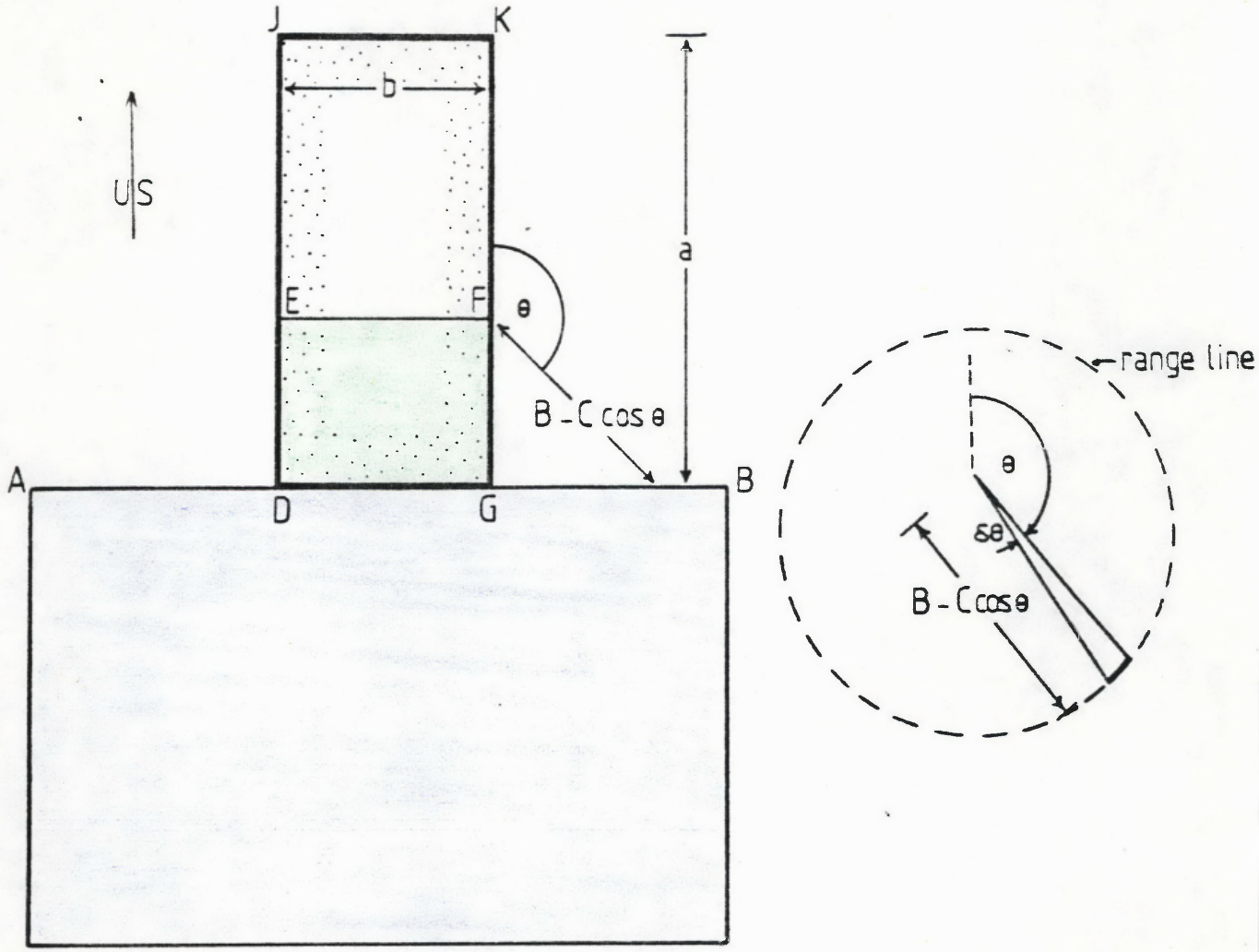

FIGURE 5.10: *Contributing region (green shading) for type 3 single boundary source/collecting area configuration. Source area, stippled; collecting area, blue shading.*

As for the type 1 configuration, this identity applies only if certain restrictions on the source/collecting area configuration are complied with. Firstly, distances AD and GB in Figure 5.10 (taking the configuration for the downslope component as an example) must be greater than $B - C\cos\theta$ when θ is close to $3\pi/2$ or $\pi/2$ respectively. Otherwise the collecting area is not large enough to include all particle displacements from the source area across AB. As there are no instances among published configurations of this restriction not being complied with, analysis of its effect on collecting rate has not been undertaken.

The second constraint is the same as that of the type 1 configuration, *i.e.* that the length of the tray must be greater than $B + C$, to avoid restriction of the contributing region by the upslope edge of the tray when θ is close to π. As some published configurations (*e.g.* that of Quansah, 1981) do not comply with this constraint, analysis of the effect on collecting rate is given below. Figure 5.11 shows that for θ changing in value from $\pi/2$ to π, the contributing region boundaries are first partly within and partly coinciding with the source area, then for $\theta = \theta_c$ the boundaries of the contributing region coincide exactly with those of the source area. For $\theta > \theta_c$ the contributing region remains coincident with the source area. The areas of the contributing regions are:

$$\pi/2 \leqslant \theta < \theta_c \ ,$$

$$\text{length EF} \times \text{length FG} = bC\cos^2\theta - bB\cos\theta$$

$$\theta_c \leqslant \theta \leqslant \pi \ ,$$

$$\text{length EF} \times \text{length FG} = a\ b \ .$$

These areas are identical with those for the type 1 analysis (Figure 5.8). As for the type 1 analysis, θ_c is given by:

$$\theta_c = \cos^{-1} \frac{B - \sqrt{B^2 + 4aC}}{2C} \ ,$$

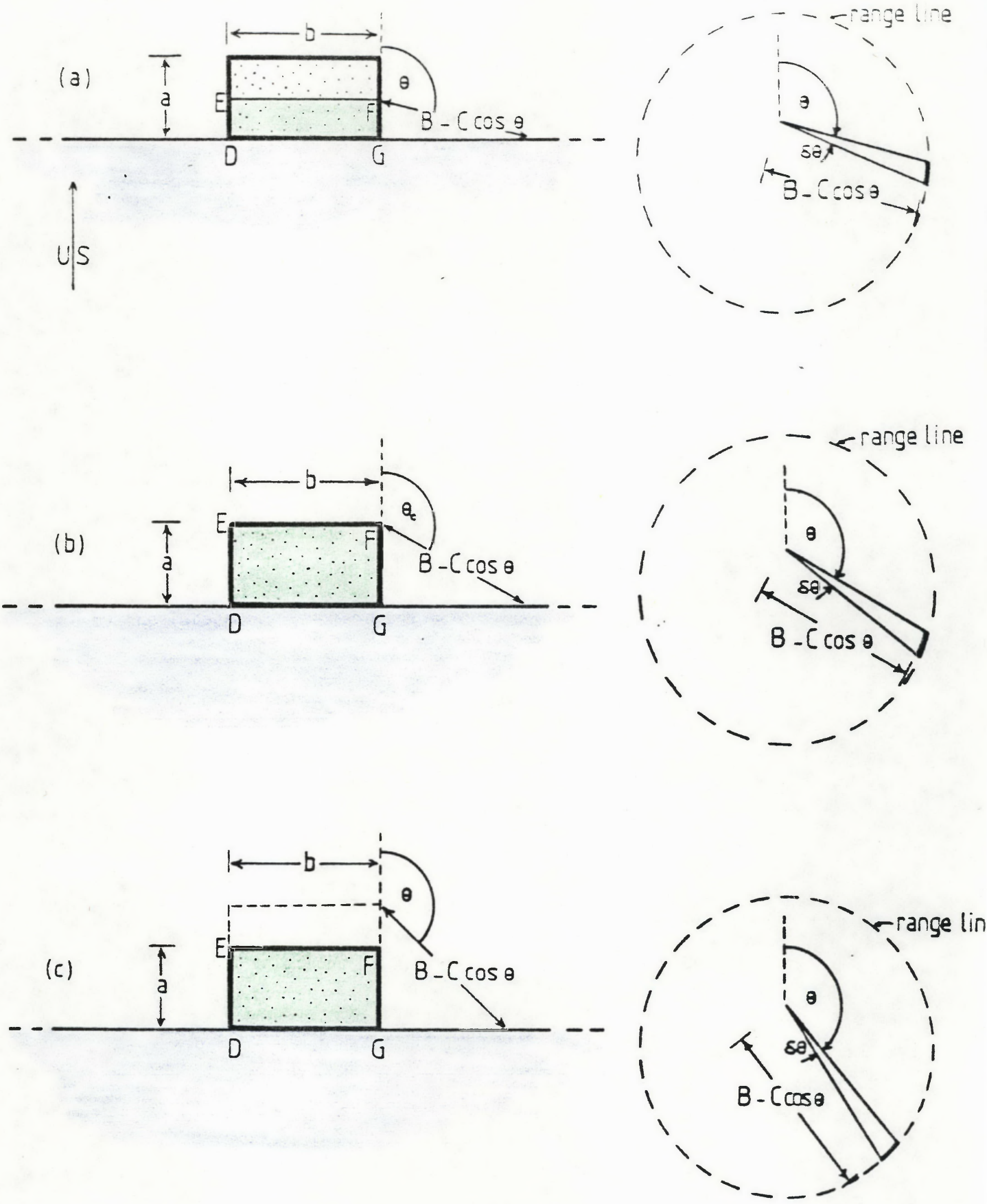

FIGURE 5.11: *Contributing regions (green shading) for type 3 single boundary source/collecting area configuration with length of source area less than the length of some particle displacements: a) $\pi/2 \leq \theta < \theta_c$; b) $\theta = \theta_c$; c) $\theta_c \leq \theta \leq \pi$. Source area, stippled; collecting area, blue shading.*

so that the collecting rate for $\theta: \pi/2 \leq \theta \leq \pi$ is also given by the lengthy expression in terms of $\cos \frac{-1B - \sqrt{B^2 + 4aC}}{2C}$, equation (5.12). The observation that this bears no meaningful relationship to the downslope component splash transport rate applies here also.

Analysis of Internal Collecting Area Configurations

This configuration consists of a narrow slit-like collecting area on the downslope side of a rectangular source area, the whole surrounded by an outer source area (Figure 5.3; Lattanzi *et al.*, 1974; Singer *et al.*, 1981). The boundary between the inner and outer source areas is an obstacle only to overland flow and allows free movement of splash. For particle displacements ($\theta: \pi/2 \leq \theta \leq 3\pi/2$) greater than the maximum collecting area dimension but less than the minimum distance between the collecting area boundary and the outer boundary of the outer source area, the contributing region is as shown in Figure 5.12. The area of this region is simply ab, so that collecting rate for displacements with a downslope component is given by the integral, I_1:

$$I_1 = \frac{im}{2\pi} \int_{\pi/2}^{3\pi/2} ab \, d\theta$$

$$= \frac{i\ m\ a\ b}{4} \ .$$

If the source/collecting area configuration were to comply with the above mentioned restrictions for all directions of displacement (which the configurations of Lattanzi *et al.* (1974) and Singer *et al.* (1981) do not) then the collecting rate, c_9, would be:

$$c_9 = \frac{im}{2\pi} \int_{0}^{2\pi} ab \, d\theta = i\ m\ a\ b \ . \qquad (5.15)$$

This is obviously directly related to m, the mass detached per drop.

If the two restrictions on the configuration dimensions are not complied with, then only part of the potential contributing region can supply

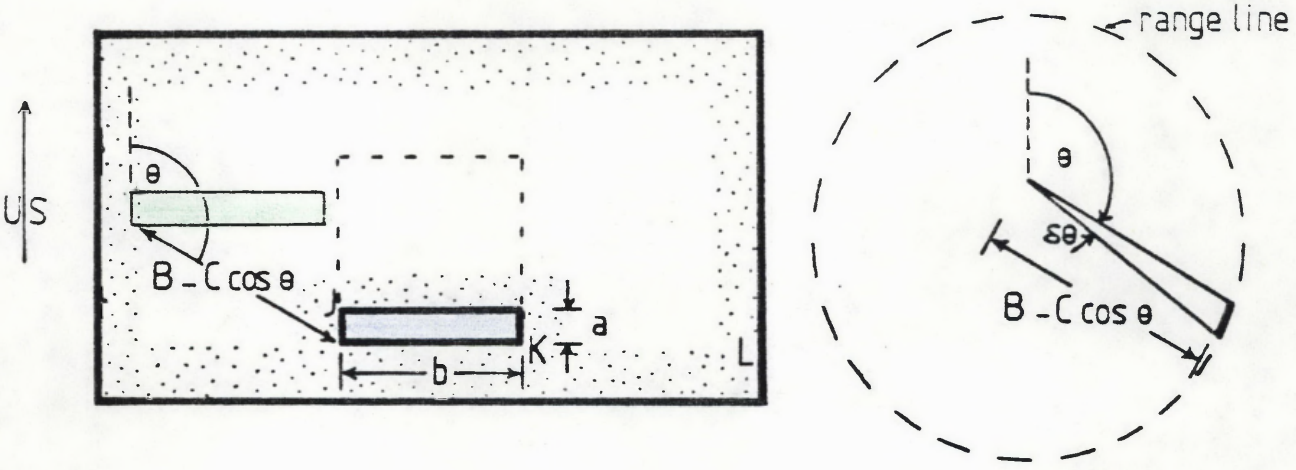

FIGURE 5.12: *Contributing region (green shading) for internal collecting area. For the configuration shown, and for the range of θ involved (θ: π/2 ≤ θ ≤ 3π/2), the maximum dimension of the collecting area is the distance between points J and K; the minimum distance between the collecting area boundary and the outer boundary of the outer source area is the distance between points K and L. Source area, stippled; collecting area, blue shading.*

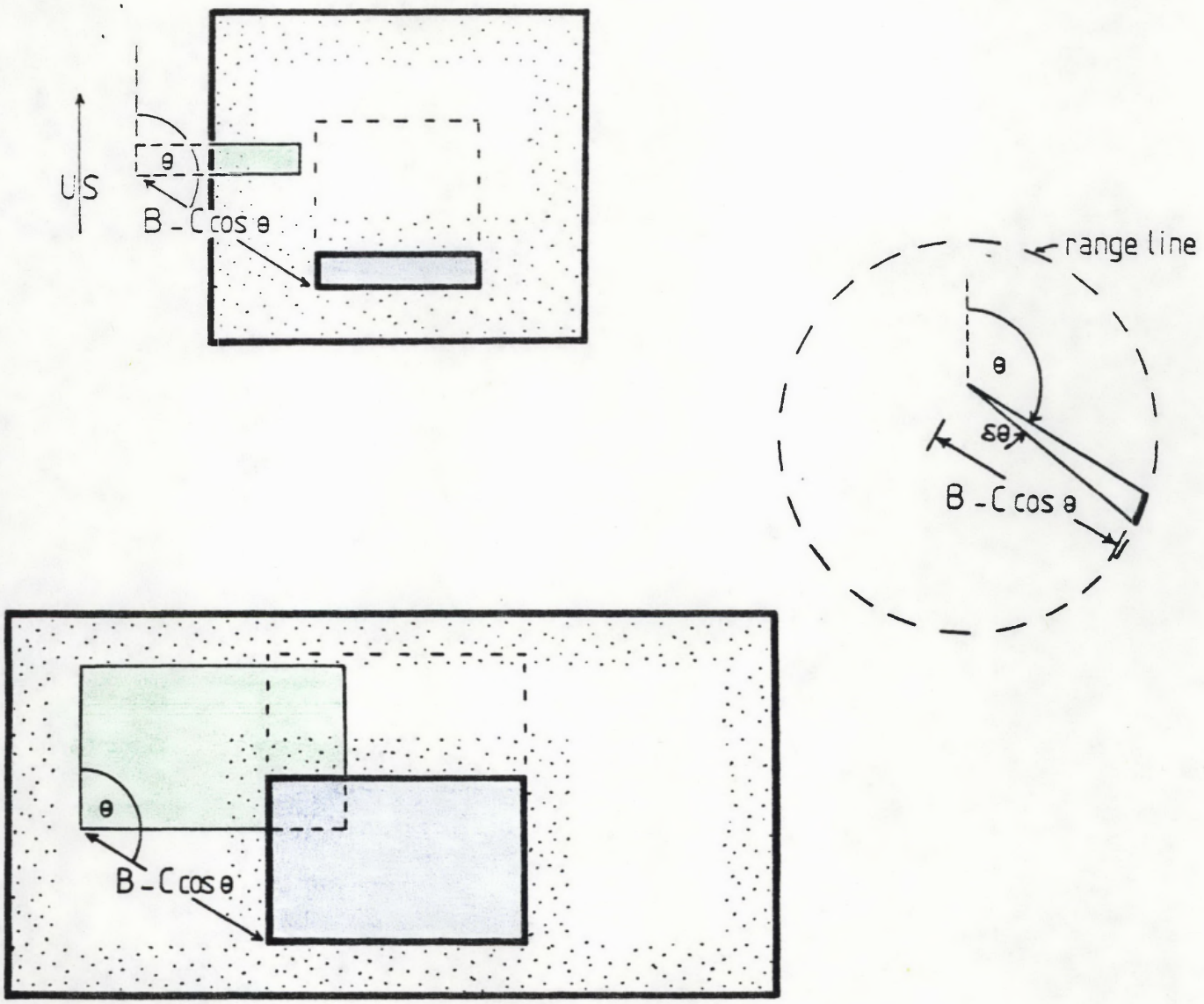

FIGURE 5.13: *Contributing regions (green shading) as part of the potential total contributing region for:*
a) particle displacement greater than minimum distance between collecting area boundary and outer boundary of outer source area;
b) particle displacement less than maximim dimension of collecting area.
Source area, stippled; collecting area, blue shading.

splashed material to the collecting area, as shown in Figure 5.13. Analysis of the effect of this on collecting rates by the methods used previously was found not to be possible without recourse to numerical solutions for roots of trigonometric equations and numerical evaluation of integrals of lengthy trigonometric expressions. In view of the small number of instances of use of the configuration this was not undertaken. It can be stated, however, that, on the basis of experience with the configurations examined so far, it is most unlikely that the collecting rate for an internal collecting area not complying with the above dimensional restrictions would show any meaningful relationship to component or resultant splash transport rates.

The Moment Method

This has been used with small trays (Savat, 1981; Poesen and Savat, 1981) and cups (Reeve and Perrens, 1980). Proofs have been given by these authors using the assumption of an exponential splash mass distribution and by discrete methods, respectively, that resultant splash transport rate can be equated to the rate of change of the first moment of mass of the source/collecting area system. A full analytical proof that requires no assumption of the nature of the splash mass or inter-rill mass distribution has been given in Section 4.3.3. No restrictions need to be placed on the source/collecting area configuration, although there are some purely practical restraints that have been discussed by Reeve and Perrens (1980) and Poesen and Savat (1981).

5.3 Field Measurement

5.3.1 Splash traps

Survey of Configurations

Published splash trap configurations are shown in Figure 5.14. These have: (i) horizontal or near horizontal collecting surfaces (Morgan, 1982); (ii) a horizontal or near horizontal collecting aperture (Bollinne, 1975; Soyer *et al.*, 1982); (iii) vertical intercepting surfaces (Ellison, 1944). Although care is taken to minimise distrubance in the field installation of splash traps, it is inevitable that resultant transport rates will change in the region of the splash trap due to a section of the soil surface

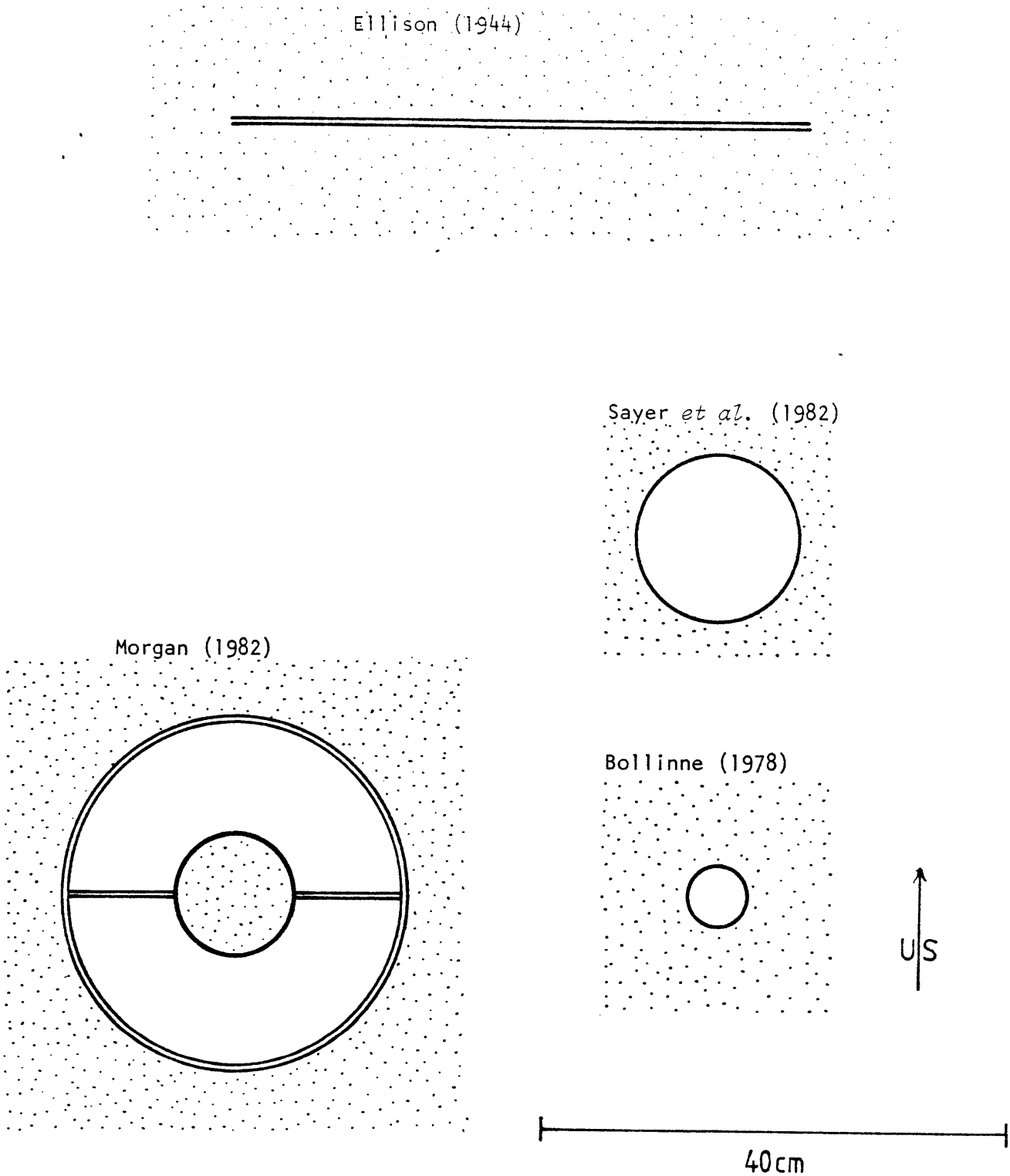

FIGURE 5.14: *Spatial configuration of source and collecting areas for field splash traps. Stippled area - source area, plain area - collecting area, single line - boundary over which splash can pass, double line - boundary over which splash cannot pass, i.e. boundary with vertical extent.*

being replaced by a surface not contributing splash. This is examined qualitatively below.

Qualitative Considerations

As for the soil tray case, the distribution of resultant transport rates on a uniform sloping soil surface is characterised by a uniform magnitude and direction of resultant at all points on the surface (Figure 5.15(a)). When, however, a portion of the soil surface is occupied by a splash trap that is acting as a sink for splashed material and not a source, then the resultant at points near the splash trap is affected by the lack of splashed material coming from the direction of the splash trap. For example (Figure 5.15(b)), points on the downslope side of the splash trap do not have as much material passing in a downslope direction, so that the resultant transport may here be in the upslope direction. Points further away on the downslope side of the splash trap, begin to have more material passing in the downslope direction, having been derived from the soil surface between the point and the downslope side of the splash trap. Thus, moving away from the splash trap in the downslope direction, the resultant is initially in the upslope direction, then zero, then in the downslope direction and increasing until its magnitude is the same as that of the resultant elsewhere on the unaffected part of the soil surface. This argument can also be applied in the remainder of the part of the soil surface surrounding the splash trap, to give a probable resultant transport rate distribution as shown in Figure 5.15(b). The role of analysis, then, is to compare the collecting rate of the splash trap with the resultant and component transport rates on the undisturbed part of the soil surface.

Analysis of Vertical Intercepting Surfaces

The contributing region for a vertical intercepting surface is shown in Figure 5.16. Its area is given by:

$$b\cos\theta\ (B - C\cos\theta)\ ,$$

so that the collecting rate of interception rate, c_{10}, for particle displacements with an upslope component is:

(a)

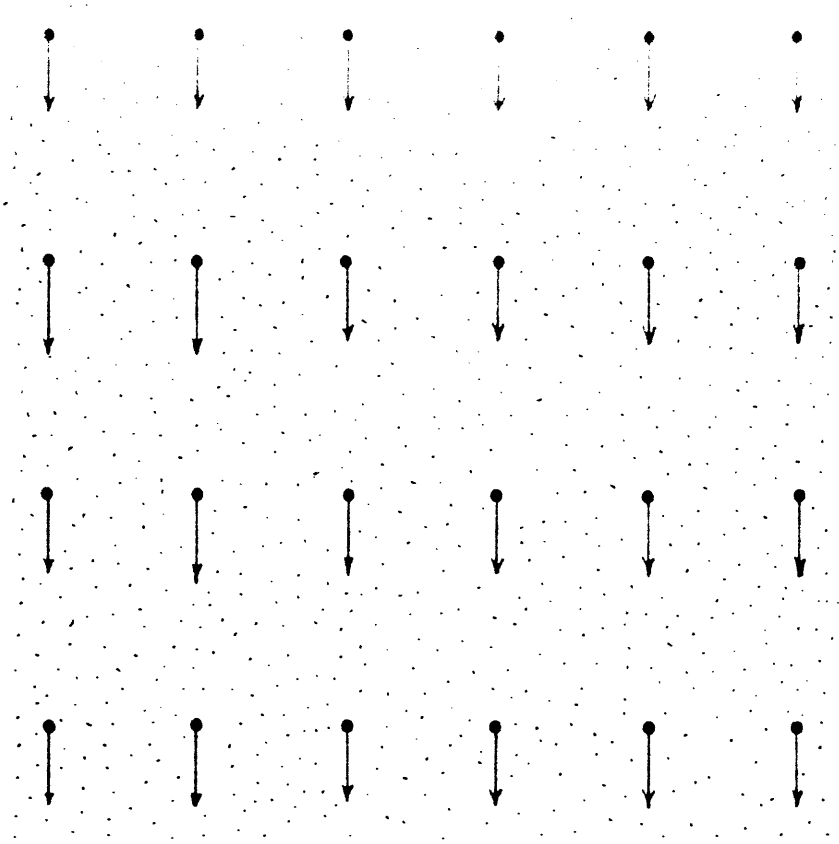

(b)

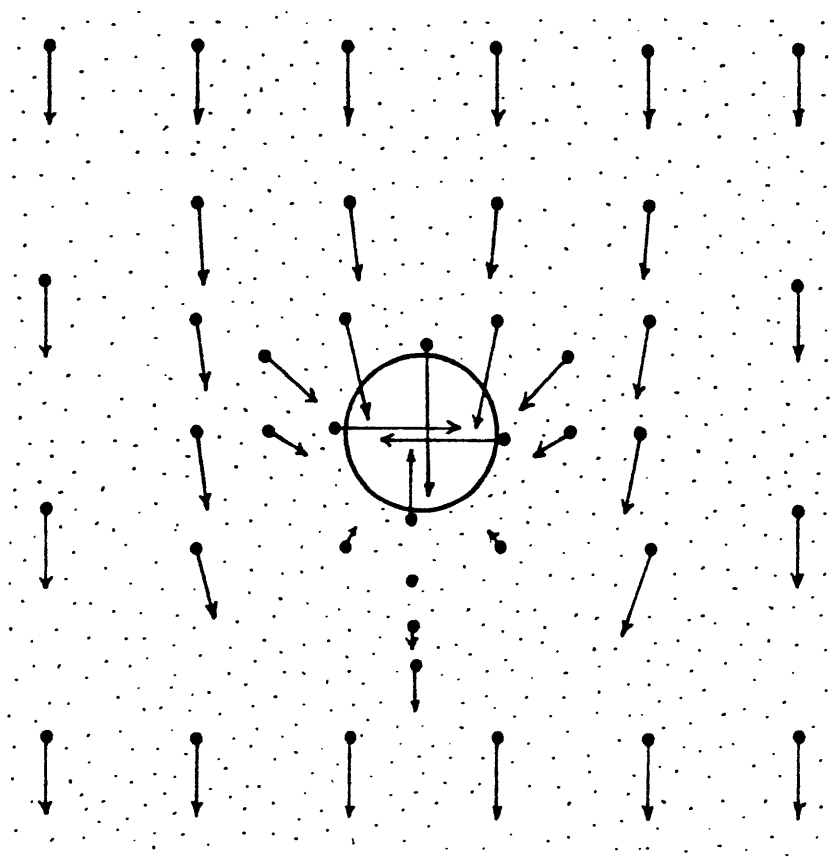

FIGURE 5.15: *Hypothetical spatial distribution of resultant inter-rill transport rates for:*
a) uniformly sloping surface of undisturbed soil;
b) the same surface with a circular sink or splash trap showing the distortion to the distribution of uniform resultants due to there being no splash derived from within the circle.

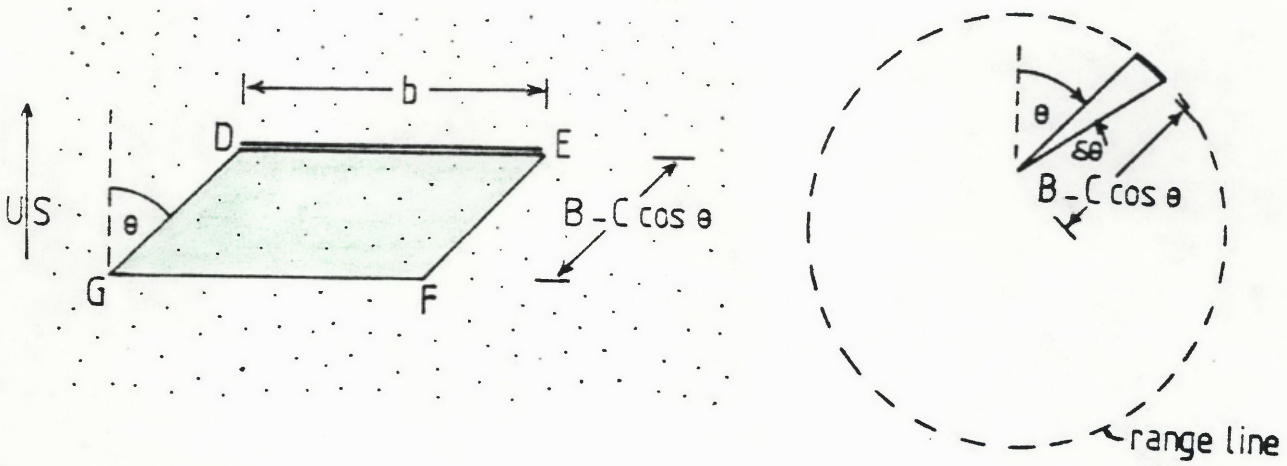

FIGURE 5.16: *Contributing region (green shading) for a vertical intercepting surface. Source area, stippled; vertical intercepting surface, double line.*

$$c_{10} = \frac{imb}{2\pi} \int_{-\pi/2}^{\pi/2} \cos\theta \, (B - C\cos\theta) d\theta$$

$$= i\ m\ b\ (\frac{B}{\pi} - \frac{C}{4})$$

$$= i\ m\ (\frac{B}{\pi} - \frac{C}{4}) \quad \text{per unit width of intercepting surface.} \tag{5.16}$$

This is identical with the upslope component splash transport rate on the undisturbed part of the soil surface. It can similarly be shown that the interception rates for vertical surfaces facing cross-slope or upslope are equal to the cross-slope or downslope component splash transport rates respectively.

Analysis of Sampling Aperture Flush With Soil Surface

The contributing region for a circular sampling aperture flush with the soil surface, and with a diameter less than the smallest particle displacement ($2R < B - C$), is shown in Figure 5.17. The area of this region is simply πR^2, so that the collecting rate, c_{11}, is given by:

$$c_{11} = \frac{im}{2\pi} \int_{0}^{2\pi} \pi R^2 \, d\theta$$

$$= im\pi R^2 \ . \tag{5.17}$$

The collecting rate per unit area of sampling aperture is therefore, im, *i.e.* the detachment rate on the soil surface. Note that equation (5.17) is the same as equation (5.1) for the collecting rate from a splash cup of diameter less than the smallest particle displacement. Each configuration is in fact the inverse of the other, the collecting area of one being the source area of the other and *vice versa*.